Kalman Filter Based Altitude Control Approach for Sea Skimming Cruise Missiles with Sea Wave Adaptation

Ozgun Dulgar, Rustu Berk Gezer and Ali Turker Kutay

Abstract Main control challenge with sea skimming cruise missiles is to achieve the lowest possible flight altitude over mean sea level during midcourse guidance phase in order to reduce its detectability against targeted warships. Contrariwise, realizing a very low altitude is a rough objective under realistic disturbances due to sea waves and measurement errors of many sensors used in the altitude control loop. Therefore, a robust altitude controller is needed to be applied to height control loop of anti-ship missiles. In this study, Kalman filter based altitude control method is proposed and compared with the existing designs in literature. Moreover, determination of the optimal flight altitude is performed by estimating the instantaneous sea condition by Kalman filter. Simulation results for widely varied scenarios, in which different sensor errors, sea conditions and discrete time applications are taken into account, are shared. Simulation results indicate that the proposed altitude control system design has pleasing performance under realistic real world conditions.

Key words: sea skimming guidance, robust altitude control, Kalman filter based estimation, sea wave optimal flight altitude

List of Abbreviations and Symbols

x	True state
x_m	Measured state
$\hat{x}$	Estimated state

Ozgun Dulgar
Roketsan Missiles Inc, 06780 Ankara, Turkey, e-mail: ozgun.dulgar@roketsan.com.tr

Rustu Berk Gezer
Roketsan Missiles Inc, 06780 Ankara, Turkey e-mail: bgezer@roketsan.com.tr

Ali Turker Kutay
Middle East Technical University, 06800 Ankara, Turkey e-mail: kutay@metu.edu.tr

x_{k-1} State at previous time step
x_k State at current time step
α Angle of attack
δ Control surface deflection
q Pitch rate
θ Pitch angle
a_z Acceleration in body-z direction

1 Introduction

Anti-ship missiles are guided missiles which have long being used in warfare on the sea against ships. Targets of these missiles are generally armed naval ships like frigates, destroyers, aircraft carriers and corvettes. Obviously, these battleships are equipped with very effective defense systems against incoming missiles, examples of most of them and far-reaching information can be found in [9]. Anti-ship missiles strongly use sea skimming guidance method to keep its existence under radar horizon of the target ship, in order to avoid detection and dodge the counter attacks. Hence, realizing a smooth sea skimming altitude profile is the major aim for an anti-ship missile.

Sea skimming guidance, by default, is achieved with altitude feedback from radar altimeter measurement. However, radar altimeters measure the height from instantaneous sea surface. This phenomenon makes the sea waves to act directly as a disturbance to the height control loop. Besides, altimeter measurement has its own noise characteristic like any other sensor output. Furthermore, altitude rate information generally cannot provided directly by an altimeter and direct derivative of the noisy altitude measurement cannot be used in height control loop. Therefore, radar altimeter measurement should be assisted with another sensor data, specifically with an accelerometer measurement, in order to obtain noise-free feedbacks to the height control loop. On the other hand, accelerometers have their own error characteristics, which also bring some problems.

There are a few comprehensive investigations about sea skimming guidance of these missiles in the literature. In 1985, Dowdle [4] proposed an altitude control system design for a supersonic low-altitude missile by using optimal regulatory theory for an ideal simulation. As already stated in that paper, many additional issues are untouched and should be considered carefully. In his second paper at same conference [5], the problem of implementing a full-state altitude control law by using Kalman filter (KF) estimations is addressed. In that work, while random noise is used as the wave disturbance, other disturbances and sensor errors are not considered. At last, he drew the conclusion that, bandwidth of the Kalman filter is bounded by both transient response requirements and instabilities induced from acceleration command in the stochastic process. In 1990, Lesieutre et al. [12] analyzed the missiles flying low over various sea states by modeling both the sea wave elevations and unsteady aerodynamics due to air/sea environment. In that paper, authors resulted

that missiles flying close to the sea may have control problems for the high sea states. In 2002, Talole et al. [18] designed a height control system by using predictive filter which reduces the effect of sea wave disturbance on the missile, significantly. In that work, sea wave disturbance is modeled as pure sinusoidal wave and other errors are not taken into account. In their following work in 2011, Priyamvada et al. [16] published a more detailed paper, exactly about the sea skimming altitude control. The authors proposed an extended state observer (ESO) based height control system which removes the sea wave disturbances by estimating the exact wave height as an extended state. But the practicality of that method was poor as not taking into account the accelerometer errors and power limitations for flight computer. In [6] published in 2016, which can be mentioned as the previous study of this work, extended Kalman filter (EKF) based altitude controller is proposed. In that paper, proposed altitude control algorithm shows satisfactory results under the existence of sea wave disturbance altimeter noise and accelerometer bias. Moreover its feasibility is proved not only in theory but also in practical usage for a digital discrete time computer. The considerations in that paper were almost in every aspect but two issues were untouched. First, altimeter rate information was assumed to be available in that paper but which actually is not. Second, missile was commanded to fly at a very safe altitude independent from the sea state, that is, wave-adaptive flight altitude determination was missing. Both issues are covered in this work.

The main difference between this study and the ones already in literature is to optimize the sea skimming flight of the anti-ship missile by means of both altitude controller and altitude commander together, with considering all the disturbances and conditions at the same time. By this way, proposed method provides more robustness against many practical problems.

Organization of the remaining of this paper is as follows. A sample pitch plane missile model with an acceleration autopilot and the ideal case height controller is introduced in Sect. 2. Some real world effects are addressed and the performance of the ideal case height controller with those real world effects is analyzed in Sect. 3. In Sect. 4, upon mentioning previous methods in literature, three-state Kalman filter based altitude controller is proposed and comparative simulation results are shared. In Sect. 5, details of the generation of the optimal flight altitude throughout different flight conditions are examined and corresponding simulation results are shared. And finally, concluding remarks are noted in Sect. 6.

2 Missile Model and Ideal Case Altitude Controller

Since the concern of this study is altitude control, pitch plane motion will be sufficient for the analysis. A sample missile schematic shown in the Fig.1 illustrates the pitch plane motion related parameters for the missile.

Detailed derivation of equations of motion and linearization of the pitch dynamics for a constant speed flying, roll stabilized and symmetric cruciform missile can

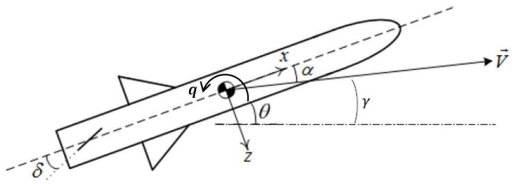

Fig. 1 Missile coordinate system and parameters

be found in numerous sources. For this study, dynamics for the pitch plane will be expressed as linear time invariant (LTI) system as in (1).

$$\begin{bmatrix} \dot{\alpha} \\ \dot{q} \end{bmatrix} = \begin{bmatrix} \frac{Z_\alpha}{mV} & \frac{Z_q}{mV}+1 \\ \frac{M_\alpha}{I_{yy}} & \frac{M_q}{I_{yy}} \end{bmatrix} \begin{bmatrix} \alpha \\ q \end{bmatrix} + \begin{bmatrix} \frac{Z_\delta}{mV} \\ \frac{M_\delta}{I_{yy}} \end{bmatrix} \delta$$
$$a_z = \begin{bmatrix} \frac{Z_\alpha}{m} & \frac{Z_q}{m} \end{bmatrix} \begin{bmatrix} \alpha \\ q \end{bmatrix} + \frac{Z_\delta}{m}\delta \quad (1)$$

In order to examine the performance of the height controller, a sample missile model should be generated. Most of the existing height control methods adopt an acceleration autopilot for their inner loop [4, 5, 12, 18, 16, 6]. Therefore, also in this work, altitude controller is designed upon the pitch acceleration autopilot. Following subsections describe by what method inner and outer loop for the altitude controller is constructed.

2.1 Pitch Acceleration Autopilot

There exist different acceleration autopilot configurations in the literature as well as different design techniques for each configuration. A well-known autopilot configuration is the full state feedback controller approach given for different applications in [15]. In this study, full-state feedback controller with an integrator is adapted to acceleration autopilot with also considering control actuation system (CAS) for fin deflection dynamics. Gains are calculated by pole placement method. Details of autopilot design process are skipped since the procedure is pretty familiar with the ones who are interested in missile control. The autopilot transfer function to be used in this study for missile cruising at 0.8 Mach is shown in (2).

$$G(s) = \frac{a}{a_{com}}(s) = \frac{-13127s^2 + 2625330}{s^5 + 215s^4 + 18744s^3 + 241732s^2 + 1274800s + 2625330} \quad (2)$$

The response of the autopilot to the step input is shared in the Fig.2. As seen, settling time of the autopilot is around 1 second, which is very common for a typical cruise missile.

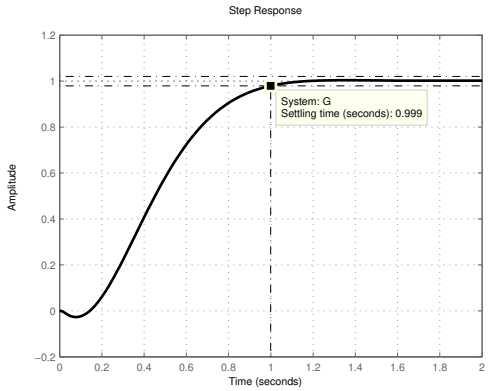

Fig. 2 Step response of the acceleration autopilot

2.2 PD Altitude Control System Design

For the sea skimming phase of the anti-ship missile, an altitude control system is needed to maintain the cruise altitude of the missile just above the sea surface. Having obtained the acceleration autopilot, now altitude controller is closed upon it. Since the level flight is the case, large body angles do not occur, so the relation between the body acceleration and altitude can be represented by a double integration as shown in the Fig.3.

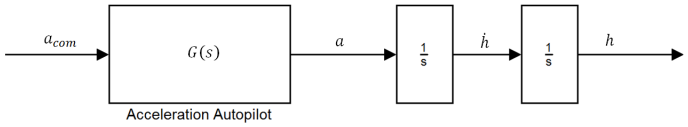

Fig. 3 Block diagram of the relation between acceleration and altitude

Then the transfer function from commanded acceleration to realized altitude can be written as in 3.

$$H(s) = \frac{h}{a_{com}}(s) = G(s)\frac{1}{s^2} \tag{3}$$

Aim of the altitude controller is to produce proper acceleration command for the autopilot, which will realize that acceleration, in order to achieve desired altitude command. The open loop system $H(s)$ above is called as a type-2 system in control theory due to the double integration in path. Such a system can be stabilized with a derivative action, by making system type-1. Thus, proportional and derivative (PD) is a proper choice for the altitude controller as an outer loop of acceleration autopilot. Feedback for the controller is provided by radar altimeter. Since radar altimeter

does not measure the altitude over mean sea level, but measures the distance over sea surface just at that moment, instantaneous wave height inherently acts as a disturbance to the system. Block diagram of the altitude controller is shown in the Fig.4.

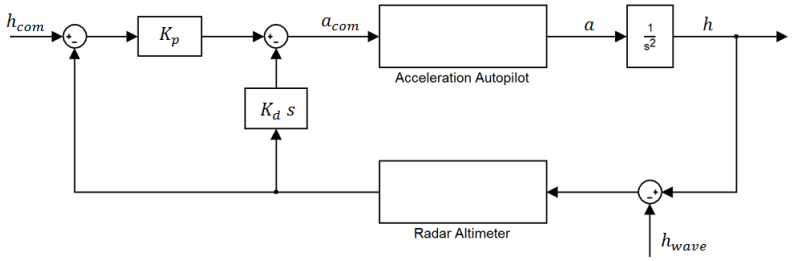

Fig. 4 Block diagram of the altitude controller

Proportional and derivative gains now should be set according to the desired performance. For the altitude control action, overshoot is unacceptable since the missile will be flown just over the sea surface. On the other hand, since the subject in this study is a cruise missile, very agile performance is not needed, so relatively slow performance for the altitude control is not a problem. Setting the gains as $K_p = 0.52$ and $K_d = 1.16$ by trial-error, provides a performance with settling time faster than 5 seconds and no overshoot criteria for altitude response. Step response of the altitude controller is shown in the Fig.5.

After deciding PD controller gains, one can write the transfer function $H_{CL}(s)$ from desired height to achieved height which is shown in (4). Similarly, considering the sea waves as a disturbance, wave rejection transfer function $H_{WR}(s)$ of the close loop system can be written as shown in (5).

$$H_{CL}(s) = \frac{h}{h_{com}}(s) = \frac{K_p H(s)}{1 + K_p H(s) + K_d H(s) s} \tag{4}$$

$$H_{WR}(s) = \frac{h}{h_{wave}}(s) = \frac{K_p H(s) + K_d H(s) s}{1 + K_p H(s) + K_d H(s) s} \tag{5}$$

Bode diagrams of the closed loop performance transfer function and wave rejection transfer function is shown in the Fig.6 as well as with the inner loop acceleration autopilot. While the closed loop bode diagram shows performance of the system by means of command tracking, wave rejection bode diagram indicates that system is vulnerable to frequencies of wave components less than 1 Hz.

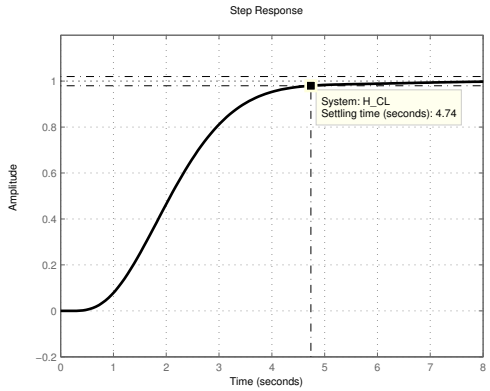

Fig. 5 Step response of the altitude controller

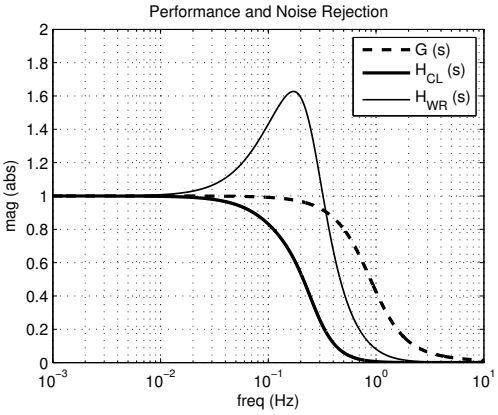

Fig. 6 Bode diagram of the altitude control system

3 Real World Effects

Performance of the height control system for the ideal feedback case will not be different from the step response shown in the Fig.5 since linear analysis is performed. On the other hand, performance analyses of the altitude controller should also be performed for realistic cases. Thus, real world effects are introduced into the simulation environment.

3.1 Sea Wave Disturbance

Modeling of sea waves has drawn considerable interest among several engineering disciplines through the last decades. Although it is completely another discipline and an area of research itself, in order to analyze the effects of sea waves on the per-

formance of sea skimming missile, a proper model should definitely be built. Sea state defines the general condition of the sea surface at a certain location and moment. Statistics about sea surface like the wave height, period and power spectrum characterizes the sea state. In oceanographic theory, there are different yet similar sea state and wave relations under the influence of wind [7]. World Meteorological Organization (WMO) definition of the sea state is the one commonly used. The other common description scales are by Beaufort and Douglas. But the most comprehensive and rooted one is the NATO sea state description, which will be used in this study. Table 1 taken from [1] shows the relation between sea state number and wave properties like significant wave height and wave period under different wind conditions.

Table 1 NATO sea state numeral table for open ocean North Atlantic

Sea State Number	Significant Wave Height (H_s) [m]		Sustained Wind Speed [knots]		Modal Wave Period (T) [sec]		Percentage Probability of Sea State
	Range	**Mean**	**Range**	**Mean**	**Range**	**Mean**	
0-1	0-0.1	0.05	0-6	0.5	-	-	0
2	0.1-0.5	0.3	7-10	3.5	3.3-12.8	6.5	7.2
3	0.5-1.25	0.88	11-16	8.5	5.0-14.8	7.5	22.4
4	1.25-2.5	1.88	17-21	19	6.1-15.2	8.8	28.7
5	2.5-4	3.25	22-27	24.5	8.3-15.5	9.7	15.5
6	4-6	5	28-47	37.5	9.8-16.2	12.4	18.7
7	6-9	7.5	48-55	51.5	11.8-18.5	15	6.1
8	9-14	11.5	56-63	59.5	14.2-18.6	16.4	1.2
> 8	> 14	> 14	> 63	> 63	15.7-23.7	20	< 0.05

There are various approaches for modeling the instantaneous wave elevations for a certain point. Further approaches for sea wave modeling can be found in several references [13, 17, 8]. In many methods, sea wave elevation can be calculated with a known spectrum function with the properties of the selected sea state.

For this study, linear wave theory is assumed and superposition of varying sinusoidal waves is considered to model sea wave elevations. Detailed procedure can be reached from the reference [8]. According to this method, wave elevation h_w at a certain point x at time t can be computed as the sum of N sinusoidal wave components as shown in (6).

In (6), ω_i is frequency, κ_i is the wave number and ϕ_i is the random phase angle of each wave component. Spectrum function $S(\omega)$ is selected as widely used Pierson-Moskowitz spectrum, which is appropriate for exhibiting fully developed seas.

$$h_w(x,t) = \Sigma_{i=1}^{N} \left(\sqrt{2S(\omega_i)\Delta\omega} \times sin(\omega_i t - \kappa_i x + \phi_i) \right) \tag{6}$$

For a certain point, time dependent wave motion for different sea states are shown in the Fig.7.

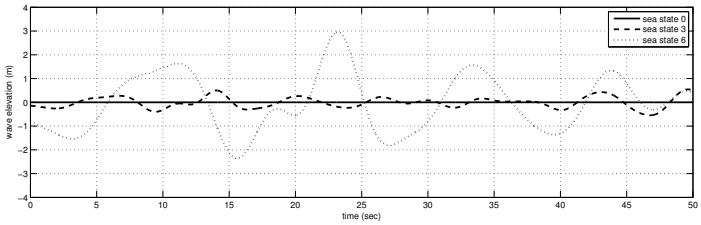

Fig. 7 Sample wave elevations for different sea states

3.2 Radar Altimeter Noise

Radio altimeter is the foremost sensor of the sea skimming missile since its output is directly used in height control loop. It measures the distance over sea surface by computing the time delay between transmitted and received radar signals. Like any other sensor, measured output of the altimeter also includes noise components which can be modeled as a Gaussian distributed white noise. For this work, RMS value of the white noise on altitude measurement is taken as 1 m as concluded in the information report in [11]. Hence, with the sea wave elevations and sensor noises, altimeter measurements can be mathematically expressed as in (7).

$$h_m = h - h_w + \eta_h; \;\; \sigma_{\eta_h} = 1m \tag{7}$$

3.3 Accelerometer Bias

Inertial measurement units (IMU) are perhaps the most important sensor on air vehicles, which measures body angular rates from the gyro and body acceleration from the accelerometer. IMU has different kinds of sensor errors, major examples of which are bias, noise, scale factor and misalignment as stated in [10]. Most effective error source among those is the sensor bias, which causes inertial navigation system (INS) algorithms to drift as time passes since integration process exists. Therefore, only the bias error for the accelerometer will be introduced to the system for performance analyses. Bias value is taken as 10 mg as a typical accelerometer bias for a cruise missile as in (8).

$$a = a + a_{bias} + \eta_h; \;\; a_{bias} = 0.1 \; m/s^2 \tag{8}$$

3.4 Limited Computer Power

In control theory, estimation techniques or observer designs are used to acquire the non-measured states. Any controller, filter or observer to be used in real applications runs on a discrete digital computer. Designer, who uses estimation or observer methods in continuous domain, should definitely consider the corresponding discrete application. Therefore, there are certain limitations with the designs, by means of filter gain limitations and observer pole locations.

For this work, onboard missile computations are assumed to run in 100 Hz discrete time, and the altimeter and IMU are considered to have measurement rates of the same.

3.5 Simulation Results with the Real World Effects

Having sorted what can the real world effects be for an altitude control problem of a sea skimming missile, now, performance analyses is performed with them. Desired height profile for the missile will be 30 meters fly-out for first 20 seconds, following with a step command to 10 meters altitude for the rest of the flight.

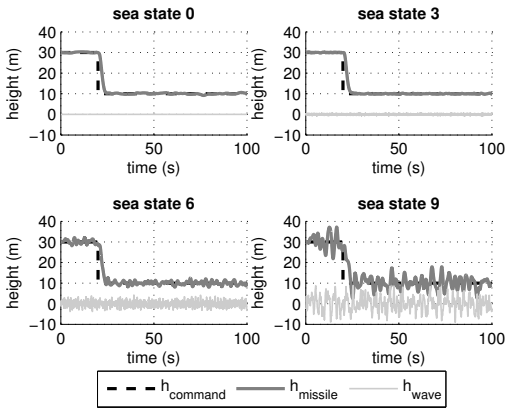

Fig. 8 Performance of the altitude controller with different sea states

In the Fig.8, performance of the altitude controller due to sea wave disturbance and altimeter noise is shown. Note that since only the radar altimeter is used in the height control loop, accelerometer bias does not affect the system, although it causes the INS algorithm to drift with time but which is an irrelevant issue for now. As expected, controller performs just well for the ideal case which is sea state 0, while the performance degrades with the increasing sea state. Undesired flight oscillation becomes significant after sea state 6, and above that, flight performance can basically said to be unacceptable. Hence, for higher sea states, more robust controller is needed.

4 Robust Altitude Control System

Having stated that a robust altitude controller for a sea skimming missile is a necessity; former studies about this specific topic are investigated. As already summarized in introduction part, there are a few studies directly analyzing this particular phenomenon. Design procedures and results for each method with each and every real world effect, are already examined and compared in [6] in detail. So, for the sake of simplicity those investigations are not repeated in this work. But still, strengths and weaknesses of commonly referred two different methods can quickly be mentioned also here as follows.

Firstly, two-state KF aided linear quadratic regulator (LQR) based altitude controller proposed in [5] works well within the effects of sea wave disturbance and altimeter noise. But since the accelerometer bias term is not included in that work, when introduced into the system, there remains a steady state bias error in the altitude response which can be seen from the results in [6]. Secondly, ESO based robust height control system proposed in [16] also does not address the problem of accelerometer bias and assumes that perfect accelerometer measurement. Although the anticipated method in that paper shows the best performance for high sea states, when the bias term in accelerometer is introduced, response of the missile drifts with time. Moreover, in that paper, pole locations at -2000 is suggested for the observer. This basically violates the Nyquist-Shannon sampling theorem stated in [14] for discrete time applications. Hence, ESO based controller also fails for the defined problem in this work.

4.1 Three-State Kalman Filter Based Altitude Controller

Both methods mentioned above are said to eliminate sea wave disturbances by aiding the altimeter measurements with accelerometer data. But neither of them considers the accelerometer bias. In fact, if the IMU measurements were perfect, there would be no need to any other sensor data since the INS solution would have been unspoiled. Therefore, while combining the data from IMU with altimeter measurement, accelerometer bias should be considered. By this motivation, re-writing the accelerometer measurement equation (8) and position, velocity, acceleration relation in discrete time, equation set in (9) is obtained.

$$a_k = a_{m_k} - a_{bias}$$

$$v_k = v_{k-1} + a_k dt$$
$$v_k = v_{k-1} + a_{m_k} dt - a_{bias} dt$$

$$h_k = h_{k-1} + v_{k-1} dt + a_k (dt^2)/2$$

$$h_k = h_{k-1} + v_{k-1}dt + a_{m_k}(dt^2)/2 - a_{bias}(dt^2)/2 \tag{9}$$

Open form of the state-space system can be written as in (10). Note that radar altimeter measures only altitude, thus, velocity measurement is missing and will be estimated through Kalman filter.

$$\begin{bmatrix} h \\ v \\ a_{bias} \end{bmatrix}_k = \begin{bmatrix} 1 & dt & -(dt^2)/2 \\ 0 & 1 & -dt \\ 0 & 0 & 1 \end{bmatrix} \begin{bmatrix} h \\ v \\ a_{bias} \end{bmatrix}_{k-1} + \begin{bmatrix} (dt^2)/2 \\ dt \\ 0 \end{bmatrix} a_{m_k}$$

$$\begin{bmatrix} h_m \\ a_m \end{bmatrix}_k = \begin{bmatrix} 1 & 0 & 0 \\ 0 & 0 & 0 \end{bmatrix} \begin{bmatrix} h \\ v \\ a_{bias} \end{bmatrix}_k + \begin{bmatrix} 0 \\ 1 \end{bmatrix} a_{m_k} \tag{10}$$

Closed form of the system in (10) can be expressed as in (11).

$$\begin{aligned} x_k &= Ax_{k-1} + Bu_k \\ y_k &= Hx_k + Du_k \end{aligned} \tag{11}$$

Having stated the system, now Kalman filter equation set, consisting of time and measurement update equations, with Joseph stabilized version of the covariance measurement update equation suggested in [3], can be written as in (12).

$$\begin{aligned} \hat{x}_k^- &= A\hat{x}_{k-1} + Bu_k \\ P_k^- &= AP_{k-1}A^T + Q \end{aligned}$$

$$\begin{aligned} K_k &= P_k^- H^T \left(HP_k^- H^T + R\right)^{-1} \\ \hat{x}_k^+ &= \hat{x}_k^- + K_k\left(y_k - H\hat{x}_k^- - Du_k\right) \\ P_k^+ &= (I - K_k H)P_k^- (I - K_k H)^T + K_k R K_k^T \end{aligned} \tag{12}$$

Once the designer choses proper Q and R matrices, Kalman filter is ready to estimate state vector $\hat{x}$. Matrix R is chosen according to the altimeter noise level and order of the accelerometer bias. On the other hand, Q matrix should be chosen by considering the desired noise level on the estimated states as well as considering the stability issues. For the calculation of Q matrix, $q = 10^{-5}$ seems to work well after trial-error runs. All in all, Kalman filter design is finalized with the selected matrices as in (13).

$$R = \begin{bmatrix} \sigma_{h_m}^2 & 0 \\ 0 & O(a_{bias}) \end{bmatrix} = \begin{bmatrix} 1^2 & 0 \\ 0 & 0.1 \end{bmatrix}$$

$$Q = Bq^2B^T = 10^{-10}\begin{bmatrix} dt^4/4 & dt^3/2 & 0 \\ dt^3/2 & dt^2 & 0 \\ 0 & 0 & 0 \end{bmatrix} \tag{13}$$

After finalizing the Kalman filter design by choosing the design parameters, the design is ready to integrate filter into height control system. Kalman filter works online in the algorithm with the height controller. External input data to the Kalman filter are the altimeter measurement h_m and accelerometer measurement a_m. States of the Kalman filter which will be estimated are; height $\hat{h}_{KF}$, vertical velocity $\hat{v}_{KF}$ and accelerometer bias $\hat{a}_{bias}$. Moreover, after estimating the altitude over mean sea level by Kalman filter, one can also obtain instantaneous wave height estimation by subtracting it from altimeter height measurement as in (14). This estimation will be used in determination of the optimum altitude process in next section.

$$\begin{aligned} h_m &= h - h_w + \eta_h \\ \hat{h}_w &= \hat{h}_{KF} - h_m \end{aligned} \tag{14}$$

Besides, recall from previous sections that, noise rejection performance of the default altitude controller was very poor from the simulation results. This is also seen from the peak in wave rejection Bode diagram in the Fig.6 which occurs at a close frequency to the bandwidth of the closed loop system and covers the similar frequency ranges. Now that, if Kalman filter estimates are to be used in height control loop, Bode diagram in the Fig.6 changes significantly and the Fig.9 is obtained. Firstly, Bode magnitude diagram of command tracking transfer function remains same; which means system performance of the designed closed loop did not change as desired. Secondly and more importantly, Bode magnitude diagram for wave rejection transfer function shifts to the left; which means, there has been an improvement in rejecting noises within considerable range of frequencies.

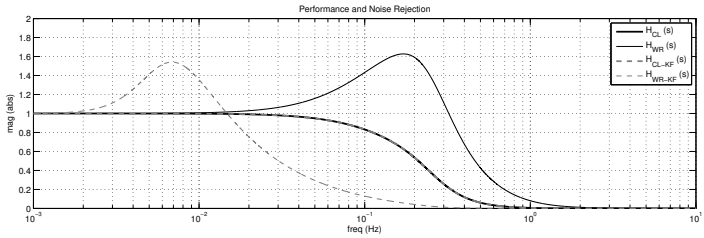

Fig. 9 Bode diagram of the altitude controller with/without Kalman filter

4.2 Simulation Results

Having designed the three-state KF based altitude controller, now it is time to compare the results with previous classical control system response shown in the Fig.8. With all the disturbances and errors included, same 4 scenarios are tested with different sea states for the new controller. Results are shared in the Fig.10.

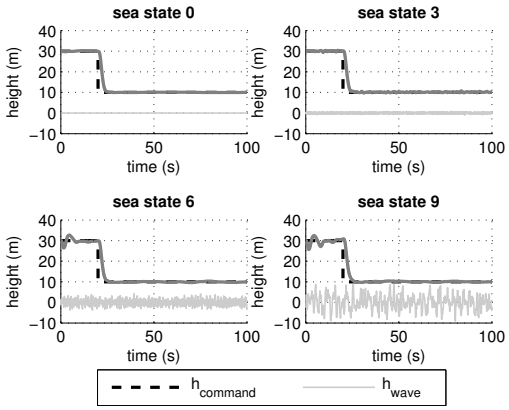

Fig. 10 Performance of the KF based altitude controller with different sea states

For the ideal case which is sea state 0, as expected, KF based controller also performs well. Similar to the performance of the classical controller in previous section, from new results it can be seen that, performance of the KF based altitude controller also degrades with the increasing sea state, especially in the beginning of the flight. There actually corresponds to transient part of the Kalman filter until full convergence in estimation, which is roughly first 5-10 seconds. But still, when the steady state performance is analyzed, even for a condition with sea state 9, command tracking is satisfactory enough. These results show that, by rejecting sea wave elevations and altimeter noise, as well as estimating the accelerometer bias, and also running in a discrete digital computer with a limited sampling frequency, proposed method 3-state KF based height control approach provide robustness against many real world effects.

5 Generation of the Optimal Altitude Profile

Importance of the sea skimming guidance strategy for an anti-ship missile is already pointed out in previous sections. If an engagement geometry and the line of sight between missile and the targeted ship on the spherical surface of the earth is considered, flying at a 3-4m altitude rather than 20m provides these missiles roughly an extra 30 seconds before detection by the targeted ship occurs, which is a huge advantage. Recall from Table 1 that sea wave elevations differ from perfect straight

sea surface to waves having above 10m height. So, at which altitude should the missile be flown is a critical problem for the controller designer. One may choose a safe altitude which covers whole sea states and disturbances, but the drawback of this easy method becomes early detection by targeted ship. On the other hand, commanding an altitude according to different sea states is possible, if sea state is known or calculated somehow at each instant.

5.1 Statistical Analyses of Wave Height

When instantaneous wave height seen by the radar altimeter as missile flying forward with 0.8 Mach speed is analyzed for a certain interval, histograms in the Fig.11 are obtained for different sea states. Shape of the histogram comes out to be very familiar, known as Gaussian distribution with zero mean.

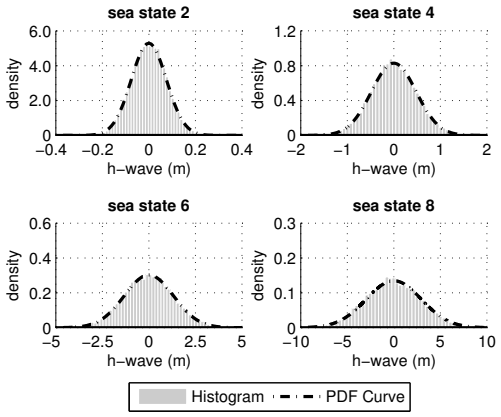

Fig. 11 Histogram of wave data and PDF curves for different sea states

Gaussian distribution, also known as normal distribution, can be defined as a two-parameter family of curves; mean μ and standard deviation σ. A general probability density function (PDF) with zero mean, as the case in sea waves, is defined as in (15).

$$PDF_{\mu=0} = \frac{1}{\sqrt{2\sigma^2\pi}} e^{x^2/(2\sigma^2)} \tag{15}$$

Cumulative distribution function (CDF) of the normal distribution is formulated as in (16). One can calculate the probability of wave height being smaller than a certain threshold by using CDF.

$$CDF_{\mu=0} = \frac{1}{2}\left(1 + erf\left(\frac{x}{\sigma\sqrt{2}}\right)\right) \tag{16}$$

CDF curves for different sea states can be seen in the Fig.12.

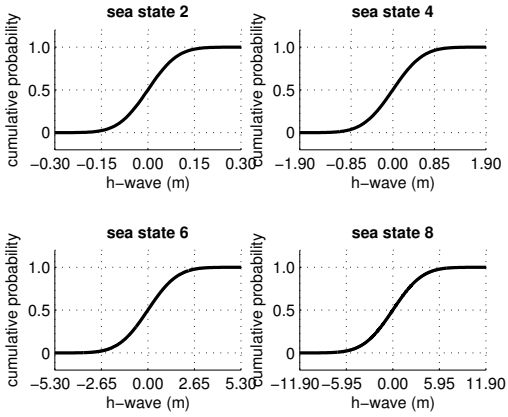

Fig. 12 CDF curves for different sea states

Inverse of the CDF is called as quantile and formulated as in 17. Quantile gives the maximum value of a variable that may have for a certain probability. Thus, one can also calculate the maximum expected wave height for a chosen probability P by this formula.

$$Q_{\mu=0} = \sigma\sqrt{2}erf^{-1}(2P-1) \tag{17}$$

Note that both CDF and Q formulas involve error function erf and its inverse. These functions do not have an analytical solution but can be solved by numerical methods. More information about error function can be found in [2].

5.2 Determination of the Optimal Flight Altitude

Having analyzed the statistics of sea wave elevations, a proper procedure for determining the optimal flight altitude should be constructed. This altitude should be robust to all the expected disturbances and errors, yet as low as it can be. Moreover, when the long flight of the missile is considered, in which missile travels hundreds of kilometers, this altitude should continuously be adapted according to the conditions involved.

Note that instantaneous sea wave elevations are not truly known by the missile computer; but the estimate is already obtained in previous section in (14). In general terms, procedure is built as follows. First of all, while flying at a higher and a safer altitude, wave estimation data will be collected for a pre-determined time interval. Then, statistical analyses will be performed through the estimated wave data. After that, according to the desired range to be covered for the next altitude command, with an acceptable risk through calculations, an altitude command will be generated. Detailed mathematical expression of this procedure is built step by step as follows.

1. Collect the wave estimation data $\hat{h}_w$ at each time step through a pre-determined time interval (sliding window #1) with period $T_{sw\#1}$ seconds, and obtain the estimated wave data array $\hat{H}_w$ with N samples.
2. At the end of the sliding window #1, having the previous wave estimation data array $\hat{H}_w$ with N samples, calculate the standard deviation σ_w of the wave height distribution by assuming mean wave elevation is zero.

$$\sigma_w(\hat{H}_w) = \sqrt{\frac{\Sigma_{k=1}^{k=N}\left(\hat{h}_w|_{@k}\right)^2}{N}} \tag{18}$$

3. From the estimated data, also calculate the characteristic wave length λ_w by counting zero-crossings z_w of the wave estimation data array with the assumption of missile is flying with an average velocity of $\bar{V}$ through time interval $T_{sw\#1}$.

$$\lambda_w = \frac{2\bar{V}T_{sw\#1}}{z_w} \tag{19}$$

4. Then define an acceptable risk of R for a single period wave. In order to correlate the optimal altitude to be calculated with the distance or time to be flown, calculate the probability P by taking into account how many periods of waves with wave length λ_w will be passed during a distance L within a time interval (sliding window #2) with period of $T_{sw\#2}$ seconds.

$$P = 1 - \frac{R}{L/\lambda_w} = 1 - \frac{R}{\bar{V}T_{sw\#2}/\lambda_w} \tag{20}$$

5. After that, obtain the standard deviation multiplier K from the new probability with the normal distribution quantile equation.

$$K = \sqrt{2}erf^{-1}(2P-1) \tag{21}$$

6. Finally, achieve a wave-safe altitude which is inside the boundaries of the taken risk by multiplying the calculated factor K with standard deviation σ_w.

$$H_{wave-safe} = K\sigma_w \tag{22}$$

7. Although a wave-safe altitude is obtained, tracking of the altitude command is never perfect in practice; hence, deviation of the missile altitude from commanded altitude σ_h should also be considered and safe altitude is obtained.

$$H_{safe} = K\sqrt{\sigma_w^2 + \sigma_h^2} \tag{23}$$

8. And lastly, altimeters working with radio signals encounter a sea clutter in very short distances; which results with invalid measurements. Hence, a bias b should also be added in order not to experience a blind range altimeter measurement.

$$H_{optimal} = b + K\sqrt{\sigma_w^2 + \sigma_h^2} \tag{24}$$

9. All in all, optimal altitude command formulation can be simplified after all previous procedures as in (25).

$$h_{opt-com} = b + \left[\sqrt{2}erf^{-1}\left(1 - \frac{4RT_{sw\#1}}{z_w T_{sw\#2}}\right)\right]\sqrt{\sigma_w^2 + \sigma_h^2} \tag{25}$$

There are three kinds of parameters in (25). Firstly, bias b and missile deviation σ_h are constants and their values are decided according to the altimeter and altitude controller performance of the missile. For this work they are taken as $b = 2m$ and $\sigma_h = 0.3m$ as the worst case. Secondly, the risk factor R and periods of the sliding windows $T_{sw\#1}$ and $T_{sw\#2}$ are design parameters of this algorithm. After some trial runs, risk factor is chosen as $R = 1\%$ and the periods of the sliding windows are chosen as $T_{sw\#1} = 10s$ and $T_{sw\#2} = 50s$. And finally, wave deviation σ_w and zero-crossings of wave data z_w are the parameters that are to be calculated online. In summary, missile will be flown along 50 seconds at the optimal altitude, which is calculated with the statistical analyses from last 10 seconds estimated wave data.

5.3 Simulation Results

Figure 13 shows the response of the missile to the commanded optimal altitude for four different sea states. As the flight environment changes by means of sea state, missile is commanded to flow at a different altitude autonomously.

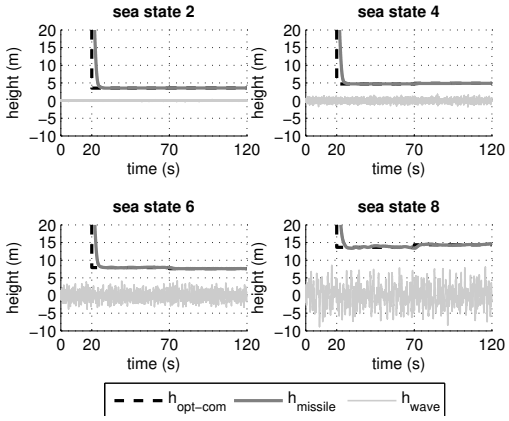

Fig. 13 Optimal altitude command and tracking for different sea states

Note that, for each separate simulation above, sea state remained constant during a single flight. In fact, effectiveness of the optimal altitude determination algorithm can better be observed for a varying sea condition. For this purpose, two other simulation conditions are created; which covers, decreasing and increasing sea state conditions. Although in nature, sea state change is not rapid, for this work, sea state is assumed to change in each 50 seconds of duration. Then, simulation results for decreasing and increasing sea states are obtained in the Fig.14. As wave elevations decrease, missile flies at a lower altitude to keep itself under target radar horizon longer. Similarly, as wave elevations increase, missile flies at a higher altitude in order not to ditch into sea. In summary, it is observed that the optimal command generation algorithm performs well by means of adapting to the sea condition. Furthermore, command tracking performance of the Kalman filter does not worsen with changing sea state, it still performs quite adequate.

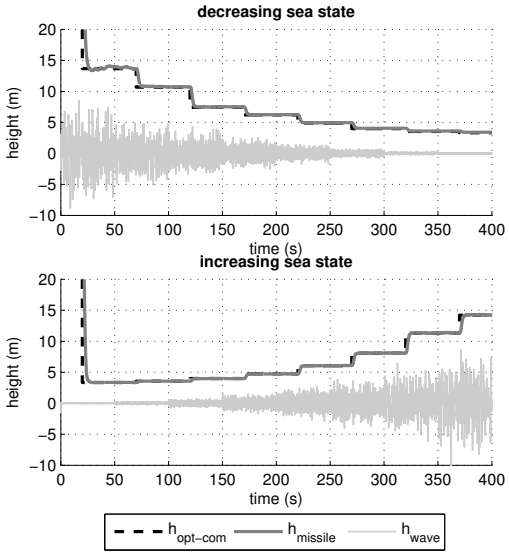

Fig. 14 Optimal altitude command and tracking for decreasing and increasing sea state

6 Conclusion

In this paper, altitude control considerations of a sea skimming anti-ship missile are addressed. First, altitude control problems due to varying real world effects are analyzed; then, a novel method is presented by means of both determining the optimal flight altitude and smooth tracking of the commanded altitude. Proposed altitude control approach displays satisfactory results. Furthermore, its applicability

is proved not only in theory, but also in practical usage within a discrete digital onboard missile computer. All in all, within the scope of addressed errors and disturbances in this work, the method presented here provides robustness to the system against many real world issues.

References

1. Bales, S., Lee, W., Voelker, J.: Standardized wave and wind environments for nato operational areas. Tech. rep., David W Taylor Naval Ship Research and Development Center Bethesda MD Ship Performance Dept (1981)
2. Clark, C.W., Olver, F., Boisvert, R., Lozier, D.: Nist handbook of mathematical functions. Cambridge University Press, ISBN pp. 978–0521192,255 (2010)
3. Crassidis, J.L., Junkins, J.L.: Optimal estimation of dynamic systems. Chapman and Hall/CRC (2011)
4. Dowdle, J.: An optimal guidance law for supersonic sea skimming. In: Guidance, Navigation and Control Conference, p. 1866 (1985)
5. Dowdle, J., Kim, P.: Bandwidth requirements for sea skimming guidance. In: Guidance, Navigation and Control Conference, p. 1867 (1985)
6. Dulgar, O., Gezer, R., Kutay, A.: Extended kalman filter based robust altitude controller for sea skimming missiles. In: AIAA Guidance, Navigation, and Control Conference, p. 1876 (2016)
7. Eluheshi, A., Matausek, M., Zatkalik, J.: Modeling of radar altimeter as the main sensor of a high performance height control of sea skimming missile flying just over a rough sea. Measurements **12**(14), 32
8. Faltinsen, O.: Sea loads on ships and offshore structures, vol. 1. Cambridge university press (1993)
9. Friedman, N.: The naval institute guide to world naval weapon systems. Naval Institute Press (1997)
10. Groves, P., GNSS, I.: Multisensor integrated navigation systems. Norwood, MA: Artech House (2008)
11. Kirby, C.: Description and accuracy evaluation of the honeywell radar altimeter. Information Report Northern Forest Research Centre (Canada). no. NOR-X-222. (1980)
12. Lesieutre, D., Nixon, D., Dillenius, M., Torres, T.: Analysis of missiles flying low over various sea states. In: 17th Atmospheric Flight Mechanics Conference, p. 2855 (1990)
13. Michel, W.: Sea spectra revisited. Mar Technol **36**(4), 211–227 (1999)
14. Ogata, K.: Discrete-time control systems, vol. 2. Prentice Hall Englewood Cliffs, NJ (1995)
15. Ogata, K.: Modern control engineering, vol. 5. Pearson Prentice Hall (2010)
16. Priyamvada, K., Olikal, V., Talole, S., Phadke, S.: Robust height control system design for sea-skimming missiles. Journal of Guidance Control Dynamics **34**, 1746–1756 (2011)
17. Ryszard, M.S.: Ocean Surface Waves: Their Physics And Prediction, vol. 11. World Scientific (1996)
18. Talole, S., Phadke, S.: Height control system for sea-skimming missile using predictive filter. Journal of guidance, control, and dynamics **25**(5), 989–992 (2002)